

Supplementary Information for

Synthesis of an unexpected $[\text{Zn}_2]^{2+}$ species utilizing an MFI-type zeolite as a nano-reaction pot and its manipulation with light and heat

Akira Oda,¹ Takahiro Ohkubo,¹ Takashi Yumura,² Hisayoshi Kobayashi² and Yasushige Kuroda^{1*}

¹Department of Chemistry, Graduate School of Natural Science and Technology, Okayama University, 3-1-1 Tsushima, Kita-ku, Okayama 700-8530, Japan.

²Department of Chemistry and Materials Technology, Kyoto Institute of Technology, Matsugasaki, Sakyo-ku, Kyoto 606-8585, Japan.

*To whom correspondence should be addressed. E-mail: kuroda@cc.okayama-u.ac.jp

(Y.Kuroda)

Additional Experimental Information

1. Comparison of the XANES data of the samples with those of the reference samples

XANES data of typical samples prepared (HMFI-Zn⁰-*X*, where *X* = 5 and 15) were compared with the spectra of both Zn²⁺MFI zeolite samples prepared using an ion exchange method in an aqueous solution of Zn(NO₃)₂ as a reference for Zn²⁺ and Zn foil as a reference for Zn⁰, as shown in Fig. S1. The XANES data of Zn²⁺ showed typical bands occurring at 9663.7 and 9669.7 eV, which are assignable to the 1*s*-4*p* transitions, whereas the data for Zn⁰ showed an alternative band occurring around 9668 eV, together with a band with broad nature in the region between 9656 and 9660 eV.

The targeted new sample, HMFI-Zn⁰-15, prepared in this work exhibited bands with a different shape in the spectrum from that of these reference samples. First, a novel strong band appeared around 9660.7 eV, which was assigned to the dipole-allowed 1*s*-σ* transition, based on the symmetrical restriction emanating from the antibonding orbital nature of σ* created from the 4*s* orbitals of the [Zn₂]²⁺ species. Second, the bands from the 1*s*-4*p* transitions of the HMFI-Zn⁰-15 sample decreased in intensity compared with the bands from Zn²⁺MFI and HMFI-Zn⁰-5. These results clearly indicate the formation of a new species in the HMFI-Zn⁰-15 sample: dimeric [Zn₂]²⁺ formed in the MFI zeolite subnanometer-sized pores through the reaction of Zn⁰ with Zn²⁺ exchanged in the MFI zeolite.

1. Examination of the validity of EXAFS analysis: Results of curve fitting procedures

To verify the results of our EXAFS analysis shown in Fig. 2, we examined the validity of the results obtained from our calculations. The resulting *k*³-weighted curves as a function of the *k* vector for the respective HMFI-Zn⁰-*X* samples are shown in Fig. S2. As can be seen, all the spectra were reproduced well by utilizing the data shown in Table 1. Therefore, we adopted these analyzed data to construct a model related to the species formed having a Zn⁺-Zn⁺ bond.

2. Comparison of the EXAFS oscillations of the samples with those of the reference samples

Depicted in Fig. S3 are the data of the FT-EXAFS oscillation of Zn K-edge for the HMFI-Zn⁰-15 sample, together with those for the reference samples: Zn-foil and Zn²⁺MFI. The band found at around 2.1 Å from the Zn⁺-Zn⁺ pair species indicates the formation of a [Zn₂]²⁺ species. It should be noted that the observed bond distance was distinctly shorter than that of the Zn⁰-Zn⁰ pair found in metallic zinc. In addition, no such band was discernible in the spectrum of the Zn²⁺MFI sample. These facts clearly support our claim that the [Zn₂]²⁺ species was formed in the MFI zeolite used as the subnanometer-sized reaction pot in our experiments.

3. The optimized structure of the [Zn₂]²⁺ species positioned at the M7-M5 site in the MFI zeolite and evaluation of its UV spectrum

To examine other possible sites that could explain the data observed in this work, we performed further DFT calculations using a model with a different Al array. In this procedure, we adopted the pairing sites connected with adjacent rings, the M7-M5 site: the M7 site comprised of 6-MR and the M5 site made up of 5-MR, in which two Al atoms occupy each ring side by side, positioned within the MFI zeolite main channel, and named the M7-M5 model: Fig. S4. Utilizing this model, a Zn²⁺ ion and a Zn⁰ atom were positioned around the M7 and M5 sites, respectively, with a separation distance of ab. 4 Å. After optimization, we succeeded in the spontaneous formation of a dimeric species, [Zn₂]²⁺, at the M7-M5 site with a stabilization energy of about -140 kJ mol⁻¹, with the bond distance converging at 2.48 Å (Fig. S4A). However, the bond distance obtained using this model is longer than both that using the M7-S2 model (discussed in the text) and the experimentally observed value of 2.35 Å.

Next, we evaluated the UV data to obtain the relation between the components from the dimer structure and the absorption characteristics in the UV-vis spectrum. The UV-vis spectrum is given in Fig. S4B, together with the component bands. The orbitals contributing to the absorption are also shown in Fig. S4B, which shows that the [Zn₂]²⁺ species has frontier orbital composed of each 4s orbital. The spectrum is reproduced well utilizing the M7-M5 model. Information on how these bands are assigned to the structure of the Zn⁺-Zn⁺ pair exchanged in the M7-M5 site is given in Fig. S4B: $\sigma-\sigma^*$, $\sigma-\pi_x$, and $\sigma-\pi_y$ transitions.

4. DFT study on the structural change of the $[\text{Zn}_2]^{2+}$ species utilizing the M7-M5 model under UV-irradiation condition

Experimentally, we observed that the activation of the Zn^+-Zn^+ species with UV irradiation creates two Zn^+ ions, as described in the main text. We also examined the DFT calculation utilizing the different model, the M7–M5 model shown in Figs. S4 and S5, which is different from that described in the main text. In this case, we assumed that excitation of the $\sigma-\sigma^*$ transition of $[\text{Zn}_2]^{2+}$ through UV irradiation creates the singlet, $[\sigma(\alpha) + \sigma(\beta)^*]$, state with the same equilibrium distance as that of the ground spin state, according to the Frank-Condon principle. The excited state formed in this way changes to the triplet state without concurrent change in the bond length between Zn^+ and Zn^+ ; we assumed the formation of the triplet state, $[\sigma(\alpha) + \sigma(\alpha)^*]$, from the excited singlet state via some kind of process as described in the text on the M7-S2 site. Thus formed triplet state then changes and forms a metastable state; two Zn^+ ions were positioned on the separated sites, respectively, because the final two stable doublet states (totally triplet state) will take the $([\text{Zn}^+(4s, \alpha)] + [\text{Zn}^+(4s, \alpha)])$ state without any interaction between the two Zn^+ ions (Fig. S5). Actually, this changing process was reproduced successfully in our DFT calculations assuming that both Zn^+ species take respective doublet states having parallel spin states, resulting in the formation of a metastable state with a Zn^+-Zn^+ distance of about 5.88 Å and a stabilization energy of ca. 2 kJ mol⁻¹, which is given by blue marks in Fig. S5-B.

On the other hand, the energy diagram of the singlet state is also depicted (red marks) as the function of distance between the Zn^+ ions, $[\text{Zn}_2]^{2+}$, which is represented by red marks. In this case, the initial state was set under the restricted condition of a Zn^+-Zn^+ distance of 5.88 Å (Fig. S5-B), with the singlet spin state (anti-parallel spin: totally singlet). By comparing the obtained energy diagram with that for the triplet state, the reverse process from two zinc ions having the same doublet spin states, $\text{Zn}^+(\alpha)$ and $\text{Zn}^+(\alpha)$ species, toward the $\text{Zn}^+(\alpha)-\text{Zn}^+(\beta)$ species with the bond length of 2.48 Å may occur if the activation energy of ca. 47 kJ mol⁻¹ at the intercrossing point (4.72 Å) can be overcome (two Zn^+ ions form a $[\text{Zn}_2]^{2+}$ species). As a result, we can explain the changing process between $[\text{Zn}_2]^{2+}$ and 2Zn^+ on the calculation level utilizing the M7-M5 site.

5. XAFS study on Sample HMFI-Zn⁰-15 as prepared and on the sample after evacuation at 873 K

The XANES data exhibit significantly different profiles for two types of sample: the sample as prepared, donated as HMFI-Zn⁰-15, and after treatment of HMFI-Zn⁰-15 at 873 K in vacuo, as shown in Fig. S6-A. The specific band-position feature of HMFI-Zn⁰-15 is the appearance of a band at 9660.7 eV, which is assignable to the 1s- σ^* transition of the dimeric [Zn₂]²⁺ species composed of two monovalent zinc ions as explained in the main text. Additional bands can be recognized at around 9663.7 and 9669.7 eV. These features are assigned to the Zn²⁺ dipole-allowed electron transitions of 1s-4p_{x,y} and 1s-4p_z.

The evacuated HMFI-Zn⁰-15 sample at 873 K shows an almost complete disappearance of the first band at 9660.7 eV, indicating a change in the state of the [Zn₂]²⁺ species formed in HMFI-Zn⁰-15. Instead, both bands occurring at 9663.7 and 9669.7 eV increase in intensity in the evacuated HMFI-Zn⁰-15 at 873 K. The disappearance of the first band and the increase in intensity of the latter two bands are interpreted as an indication of the transformation of Zn⁺ to Zn²⁺, accompanied with the formation of zinc as an atomic species through evacuation at 873 K; i.e., [Zn₂]²⁺ → Zn²⁺ + Zn⁰. This interpretation is confirmed by direct comparison with the XANES data of Zn²⁺MFI-95, as well as HMFI-Zn⁰-5, given in Fig. S1. This view is also supported by the FT-EXAFS data: the distinct band occurring at 2.1 Å was almost completely absent after evacuation at 873 K, together with an increase in the first band occurring at around 1.5 Å: Fig. S6-B. The analyzed data are summarized in Table S1.

6. ESR study in the UV irradiation process of HMFI-Zn⁰-15.

The suitable energy region for the activation of the [Zn₂]²⁺ species by irradiation using UV light with various wavenumbers was examined by detecting the formation of the ESR-active Zn⁺ species, having the electronic structure of 3d¹⁰4s¹, as shown in Fig. S7-A. In addition, in Fig. S7-B, the evaluated band-area for the Zn⁺ species formed is plotted versus the wavenumber used for activation on irradiation. As a result, the following points should be noted: it is more than the wavenumber value of 40,000 cm⁻¹ that the activation takes place efficiently. Therefore, we conclude that irradiation corresponding to the σ - σ^* transition due to the [Zn₂]²⁺ species leads to the efficient dissociation of the Zn⁺-Zn⁺ bond in the [Zn₂]²⁺ species which is ESR

silent because of the formation of a $\sigma(4s^2)$ -bond, resulting in the formation of two Zn^+ species which is ESR active species: $[Zn_2]^{2+} \rightarrow 2Zn^+$.

Table S1. A. Oda, et al.,

Sample	1st shell			2nd shell		
	$N_{\text{Zn-O}}$	$R_{\text{Zn-O}}$	$\sigma^2_{\text{Zn-O}}$	$N_{\text{Zn-Zn}}$	$R_{\text{Zn-Zn}}$	$\sigma^2_{\text{Zn-Zn}}$
(A)	2.3	1.94	0.013	1.1	2.37	0.009
(B)	2.9	1.95	0.012	0.43	2.35	0.012

Table S1. Structural parameters obtained by the EXAFS analysis for the HMFI-Zn⁰-15 sample: (A) just after preparation, (B) followed by the re-evacuation at 873 K. All measurements were carried out at 300 K.

Figure S1. A. Oda, et al.,

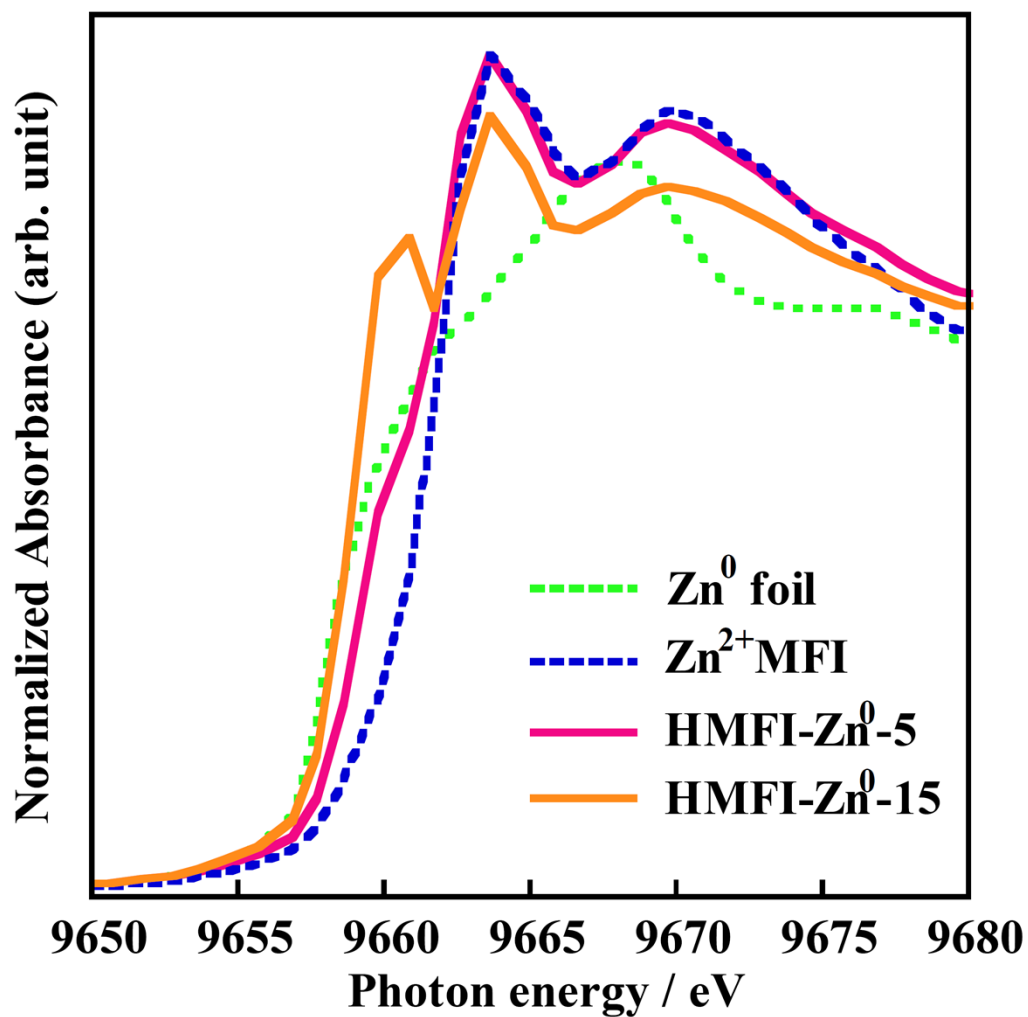


Fig. S1. XANES spectra measured for (1) the HMFI-Zn⁰-5 and -15 samples and (2) the Zn²⁺MFI sample prepared by the conventional method, and also for the reference material: Zn-foil.

Figure S2. A. Oda, et al.,

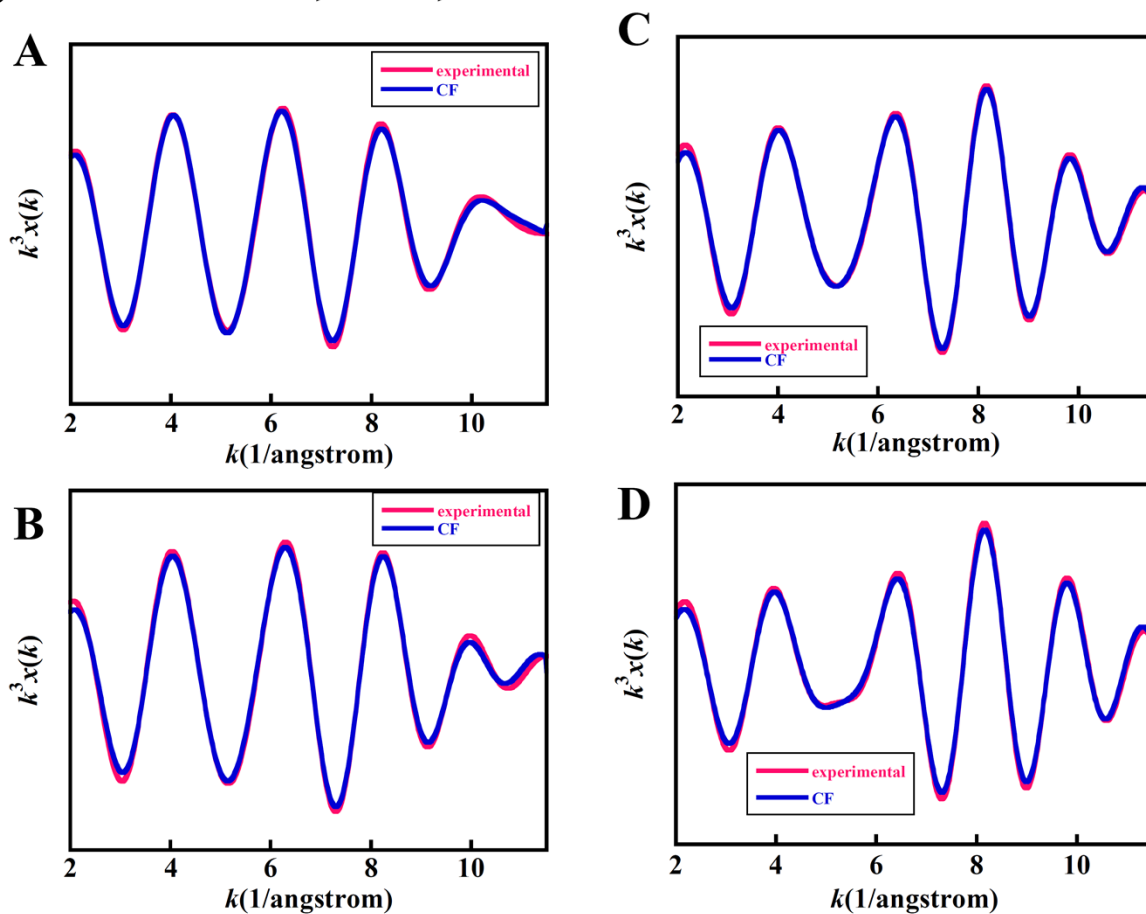


Fig. S2. The k^3 weighted $\chi(k)$ curves are given as a function of wave-vector; the experimentally obtained curve (pink) and the best-fitted one (blue) for respective HMFI-Zn^{0-X} samples by applying the evaluated parameters shown in Table S1. (A) HMFI-Zn⁰⁻⁵, (B) HMFI-Zn^{0-7.5}, (C) HMFI-Zn⁰⁻¹⁰ and (D) HMFI-Zn⁰⁻¹⁵, respectively.

Figure S3. A. Oda, et al.,

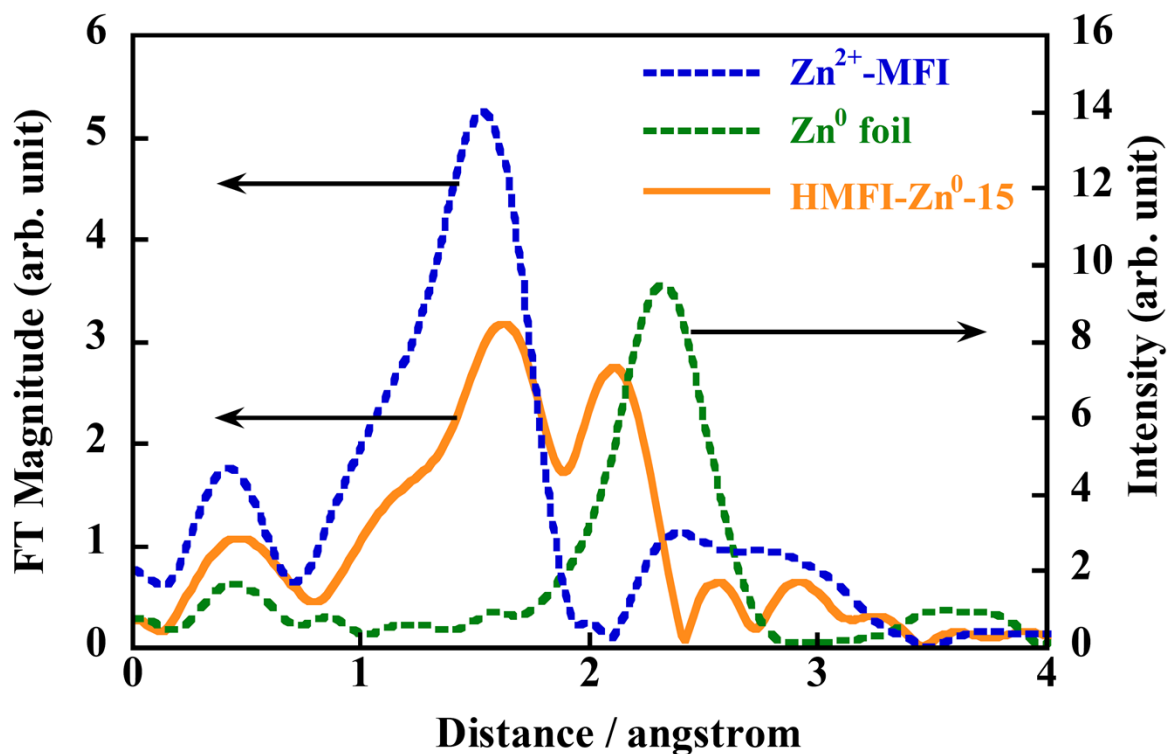
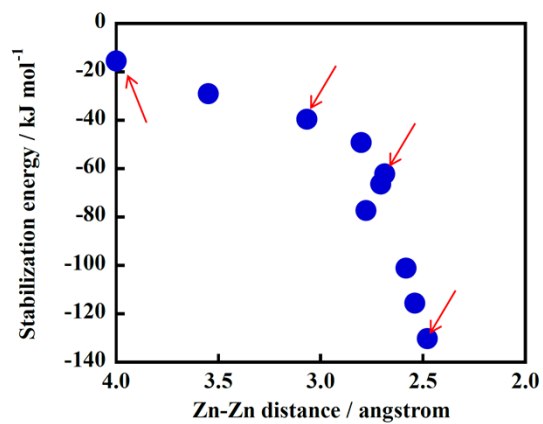


Fig. S3. Comparison of Fourier transforms of the EXAFS oscillations at the Zn K-edge among respective samples: Zn²⁺MFI, Zn-foil and HMFI-Zn⁰-15.

Figure S4-A. A. Oda et al.,



Zn_2^{2+}
formation
process on
the M7M5 site

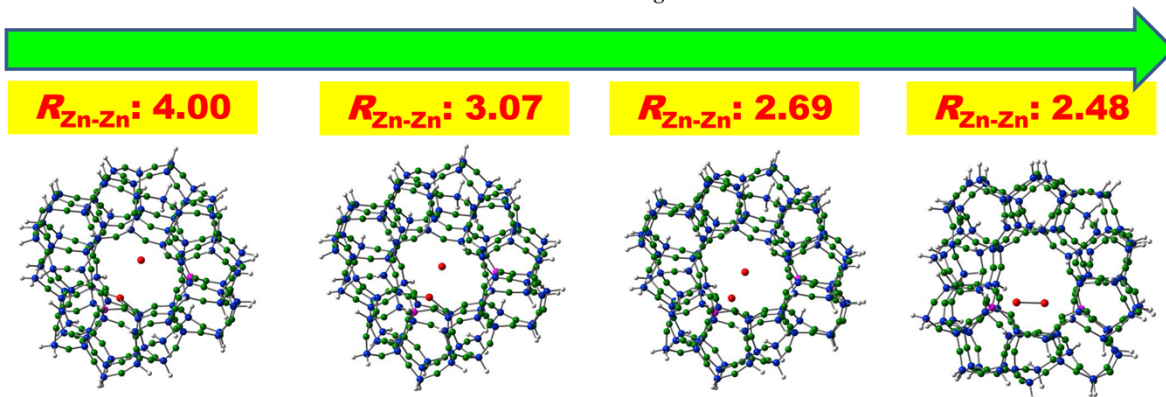


Figure S4-B. A. Oda et al.,

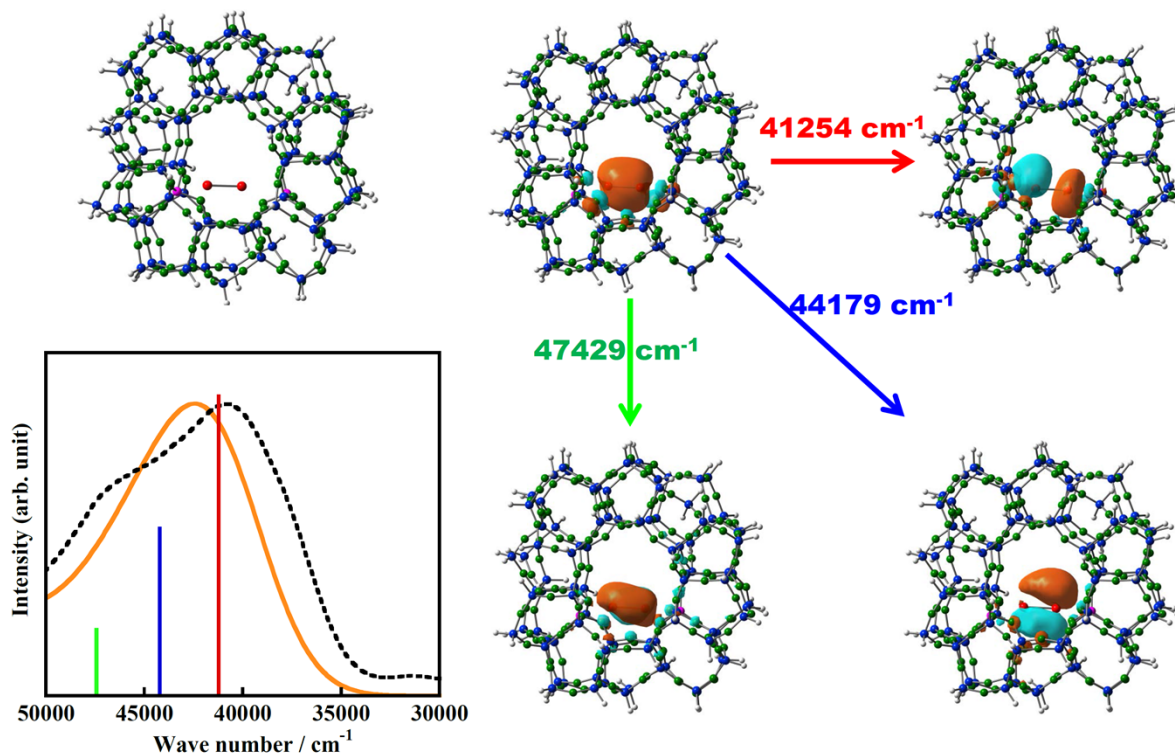


Fig. S4. (A) The optimized structure of the $[\text{Zn}_2]^{2+}$ species grafted on the M7-M5 site in MFI, as well as the stabilization energies in the respective stages, and (B) theoretically obtained components (red, blue, and green lines), and also the spectrum (orange line), by applying TD-DFT calculation method to this model, together with the experimentally obtained UV spectrum of the HMFI-Zn⁰-15 sample (dashed line). In the calculation of the spectrum by the TD-DFT method, the FWHM of the reproduced spectrum was set to $2,000 \text{ cm}^{-1}$. Their respective components corresponding to each transition from σ to σ^* , π_x and π_y , were also given; the resultant wave-numbers for three transitions are also shown.

Figure S5-A. A. Oda et al.,

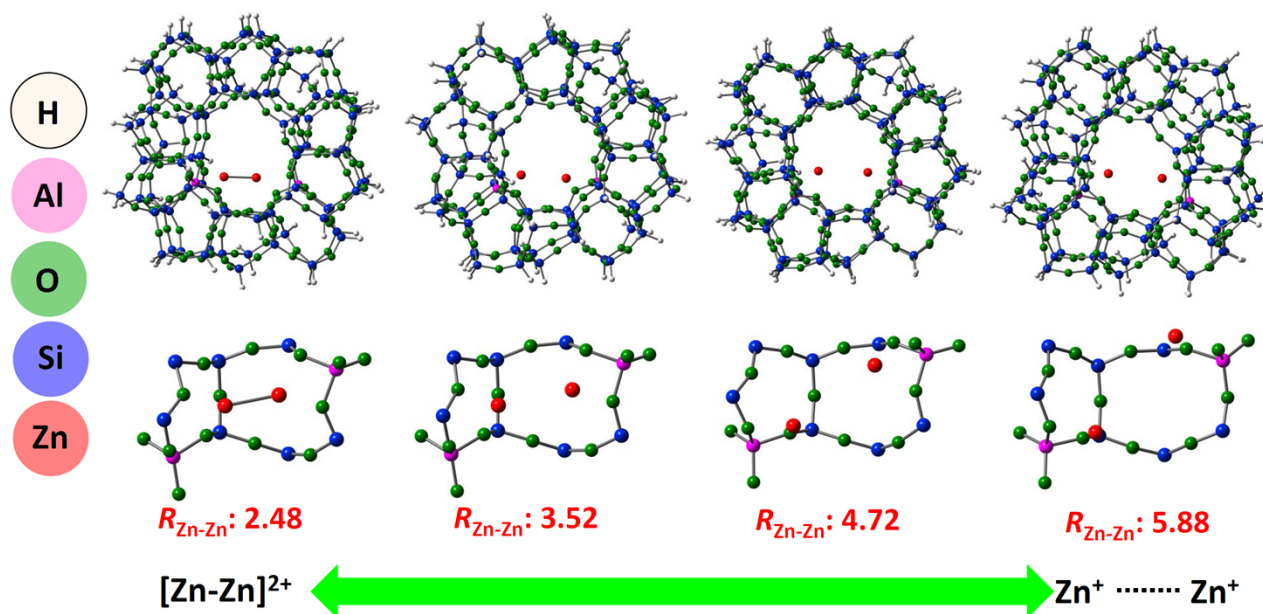


Figure S5-B. A. Oda et al.,

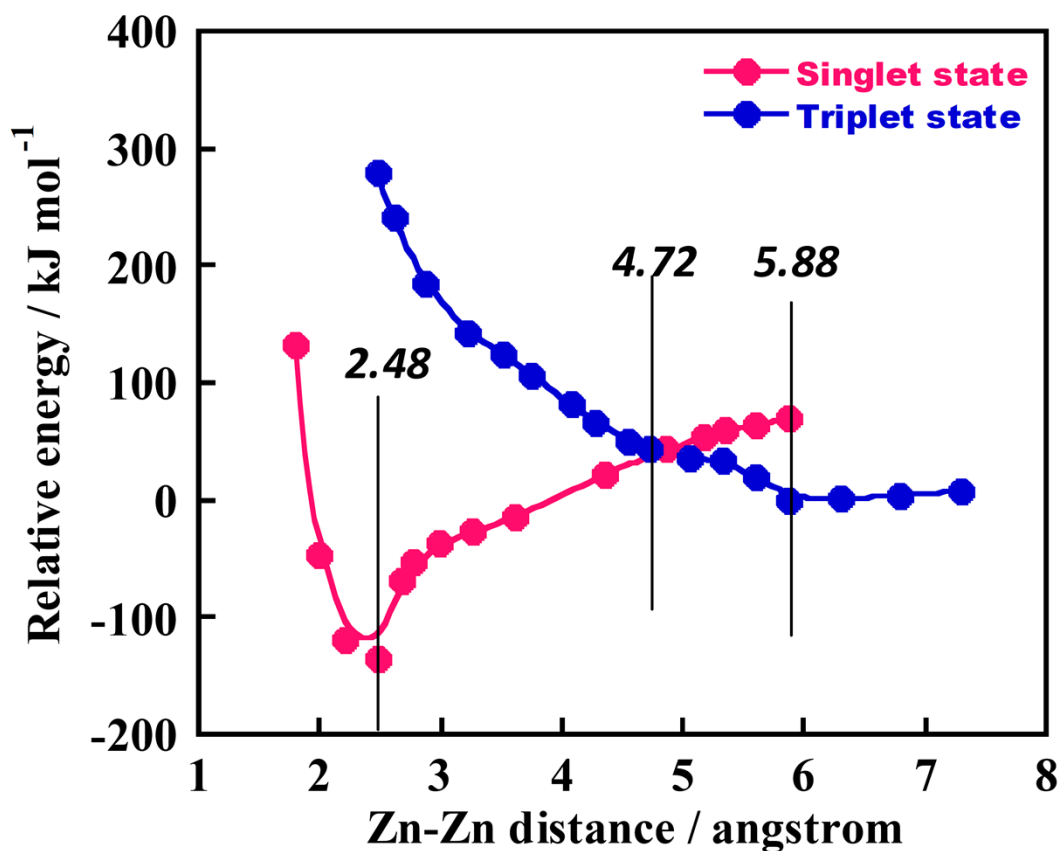


Fig. S5. The results of the DFT studies on the reversible processes between $[\text{Zn}_2]^{2+}$ and 2Zn^+ utilizing the M7-M5 model: homolysis of the Zn^+-Zn^+ bonded species, $[\text{Zn}_2]^{2+}$, in MFI or their recombination process. (A) The structures in various stages with the different Zn-Zn separation on the different model from that described in the text: the $[\text{Zn}_2]^{2+}$ species grafted on the M7-M5 site in MFI. (B) The potential energy surface of the singlet and triplet states of the $[\text{Zn}_2]^{2+}$ species evaluated by utilizing the M7-M5 model as a function of the Zn-Zn distance.

Figure S6. A. Oda et al.,

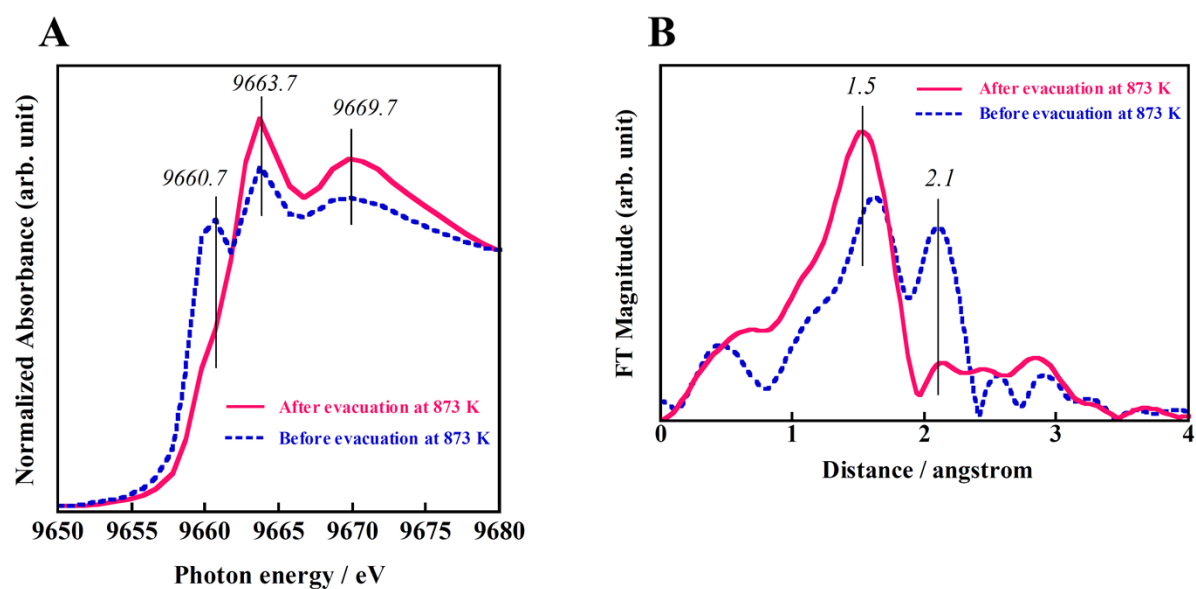


Fig. S6. XAFS study on the HMFI-Zn⁰-15 sample as prepared and on the sample after treating at 873 K in vacuo. (A) The normalized XANES spectra at the Zn K-edge. (B) Fourier transform of EXAFS oscillations of the samples treated under different conditions.

Figure S7. A. Oda et al.,

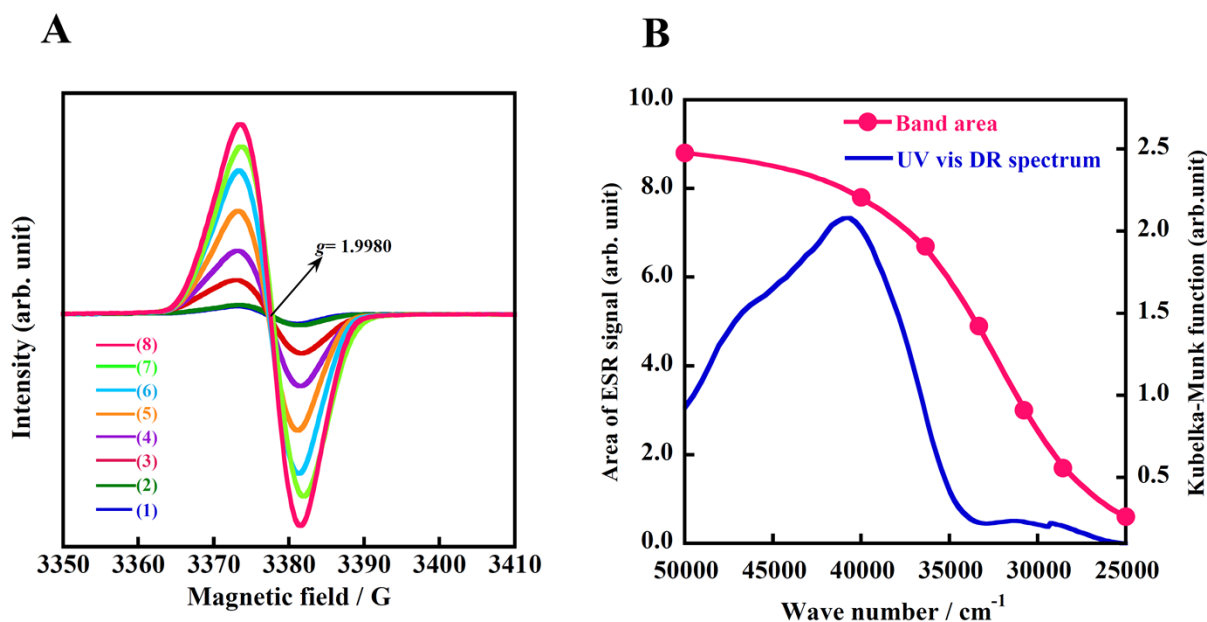


Fig. S7. (A) ESR spectra of the sample after irradiation with UV-Vis light in the various wave-number ranges. The observed ESR band is attributable to the Zn^+ species. The HMFI- Zn^0 -15 sample just after prepared, (1), followed by irradiation with light having different wavenumbers lower than (2) 25,000, (3) 28,600, (4) 30,800, (5) 33,300, (6) 36,300, (7) 40,000 and (8) 50,000 cm^{-1} , respectively. (B) Band areas of this ESR signal corresponding to the respective spectra shown in (A) were plotted against the wavenumber of irradiated light, together with the absorption spectrum of the HMFI- Zn^0 -15 sample (blue solid line).